Scaling of the Splash Threshold for Low-Viscosity Fluids

Cacey S. Stevens

The James Franck Institute and Department of Physics, The University of Chicago, Chicago, Illinois 60637, USA

arXiv:1403.3145v1 [cond-mat.soft] 13 Mar 2014

PACS 47.20.Ma – Interfacial Instabilities
PACS 47.55 D- – Drops and Bubbles

Abstract – The ambient gas pressure is determined for the onset of splashing of low-viscosity liquid drops on smooth dry surfaces as we change the control parameters: drop impact velocity, drop radius, viscosity, surface tension, density, and gas molecular weight. This threshold pressure indicates that there are two distinct regimes when drop impact velocity is varied. By rescaling data using functions of only three dimensionless numbers, the commonly used Reynolds and Weber numbers, as well as the ratio of drop radius to gas mean free path, all data is collapsed to a single curve that encompasses both regimes.

Introduction. – After years of study, physicists and engineers are still presented with a task of great difficulty: to provide criteria for the outcomes of drop impact in terms of all possible control parameters. For the case of a liquid drop impacting a smooth dry surface, the drop may bounce, spread on the surface, or splash, emitting many smaller droplets [1, 2]. The velocity of impact and drop size, as well as liquid properties (viscosity, density, and surface tension) and surface roughness, have long been known to influence the outcome [3]. Investigators have proposed conditions for the onset of splashing based solely on these parameters [4–7]. These are commonly expressed as functions of dimensionless numbers so that the criteria can lead to an understanding of the underlying mechanisms. However, there is little agreement among the proposed criteria, and they often contradict one another [8].

Only a few experimental studies of the splash threshold include the ambient gas pressure, P, which surprisingly is a crucial parameter for creating a splash [9–12]. Once P is below a threshold value, a drop no longer splashes but spreads smoothly on the surface. Accordingly, splash criteria should include P and gas molecular weight. Threshold pressure values reveal distinct regimes that occur at different values of surface roughness, liquid viscosity μ_L, and impact velocity u_0 [9, 10, 13, 14]. Therefore, splash criteria need to be determined for each regime separately.

Notably, Xu *et al.* [9] developed a splash criterion that described drop impact in the regime occurring at low-μ_L and high-u_0. However, the measurements reported here expose a discrepancy in that scaling collapse when surface tension is varied; thus a different scaling of the splash threshold for low-μ_L drop impact is presented. All splash threshold data, at both low and high u_0, collapse cleanly onto a single curve when rescaled by three dimensionless numbers. The gas mean free path is important when describing the role of ambient gas in the collapse. This master curve suggests a crossover between the low-u_0 and high-u_0 behavior and reveals different splash criteria for these two regimes.

Experimental details. – Experiments were conducted with ethanol, fluorinert, water-glycerol mixtures, and silicone oils with viscosities μ_L ranging from 0.5 mPa s to 2.7 mPa s, densities ρ_L ranging from 750 kg/m^3 to 1860 kg/m^3, and surface tensions σ ranging from 16 mN/m to 67 mN/m. I filmed drops of radius R from 0.8 ± 0.05 mm to 2.0 ± 0.1 mm using a high speed camera (Phantom V12) as drops were released inside a transparent chamber from 0.15 m to 1.5 m above dry smooth glass slides (Fisher brand cover glass). As shown previously [4, 12], the drop shape upon impact affects the subsequent splash formation. For example, drops that were oblate just before impact were more likely to splash. Therefore, only the impact of drops with a distortion in aspect ratio of less than 5% from the spherical shape were considered in the results reported here.

The average surface roughness of the glass substrate is about 5 nm, measured using an atomic force microscope [15]. A new glass slide was used for each drop impact to avoid contamination from residual liquid of previous splashes. Side views recorded with the high-speed camera were used to determine the radius R and impact velocity u_0. Each measurement was repeated 4-8 times to confirm

reproducibility. P was varied from 5 kPa to 101 kPa with one of three gases in the chamber: Helium (He), air, or Sulfur hexafluoride (SF_6). The gases have viscosities μ_G from 15.6 μPa s (SF_6) to 19.8 μPa s (He) and molecular weights m_G from 4 Daltons (He) to 146 Daltons (SF_6) [16]; μ_G does not vary with P over the range studied.

Splash threshold collapse. – As a drop impacts a smooth surface, it ejects a liquid sheet which then breaks up into droplets (see left column of Fig. 1(a)). No droplets emerge after impact if P is below a threshold value; in that case, the drop simply spreads on the surface. The boundary between splashing and spreading, shown in the right column of Fig 1(a), is defined in terms of a threshold pressure P_T, the pressure at which we first see the sheet break up into droplets. The inset of Fig. 1(b) shows P_T versus u_0 for 1.7 mPa s silicone oil drops in an atmosphere of air (▲) and in an atmosphere of SF_6 (▽). As with previous experiments [9], there are two regimes in u_0. Initially P_T decreases rapidly with u_0 to a minimum value at u_0^*. Above u_0^*, P_T increases then gradually decreases with u_0. P_T measurements in SF_6 are only shifted to lower pressures. Data in both u_0-regimes fall onto a single curve when plotted in terms of a scaled pressure, $P_T(m_G/m_{air})^{0.5}$, as shown in the main plot of Fig. 1(b). This is the same scaling as was found by Xu *et al.* [9].

In Fig. 2(a), P_T versus u_0 is shown as control parameters are systematically changed: R, μ_L, σ, ρ_L, and m_G. All data sets display the same qualitative shape; curves simply move along the P_T and u_0 axes.

All data in both regimes of u_0 fall onto a single curve when the u_0 and P_T axes are rescaled by functions of R, μ_L, σ, ρ_L, and m_G (see Fig. 2(b)):

$$u_{scaled} = u_0 \mu_L^{0.4} R^{0.3} \rho_L^{0.5} \sigma^{-0.5} \tag{1}$$

$$P_{scaled} = P_T \mu_L^{0.4} R^{0.5} \rho_L^{-0.5} \sigma^{-0.1} m_G^{0.5} \tag{2}$$

Each parameter was treated separately, leading to the scaled u_0 and P_T axes. It is challenging to find a rescaling of axes as a unique expression of all control parameters. The experimental range of each parameter is limited, and there are slight fluctuations in the data. Though not unique, these expressions lead to a good collapse of all data, over the obtainable range of the parameters.

It is insightful to find a scaling in terms of dimensionless numbers. The liquid properties, impact velocity, and drop radius can be expressed as dimensionless numbers: the Reynolds number (Re=$\rho_L R u_0/\mu_L$) giving the ratio of inertial to viscous forces and the Weber number (We=$\rho_L R u_0^2/\sigma$) giving the ratio of the inertial to surface tension forces. These experiments covered the range of $580 < \mathrm{Re} < 13100$ and $100 < \mathrm{We} < 2140$.

Another dimensionless parameter is introduced to encompass gas properties: the ratio of drop radius to the gas mean free path, R/ℓ. Note that P and m_G are expressed

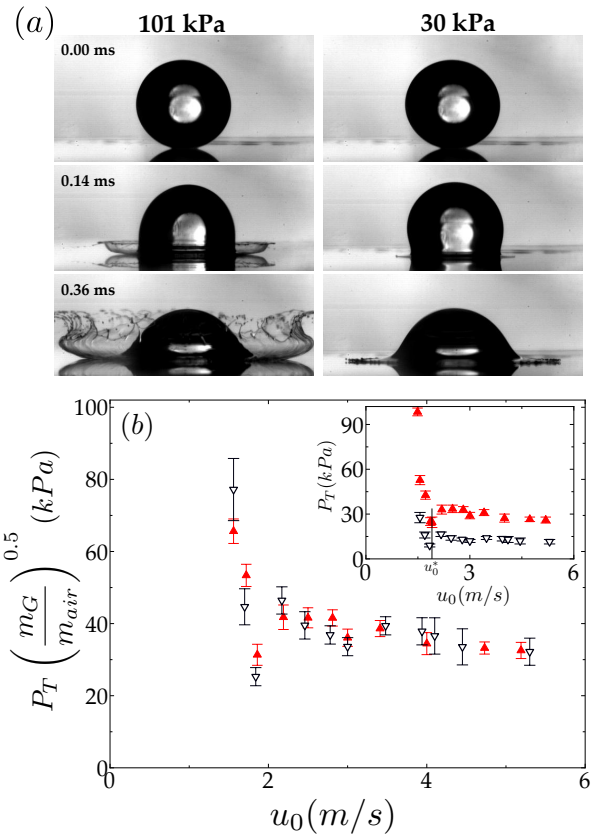

Fig. 1: (a) A 1.7 mPa s silicone oil drop is shown impacting smooth glass at 101 kPa (left) and near P_T at 30 kPa (right). Splashing is suppressed at low pressures. (b) *Inset*: P_T vs. u_0 of silicone oil drops (R = 1.6 ± 0.1 mm, μ_L = 1.7 mPa s) in an atmosphere of air (▲) or SF_6 (▽). The error bars indicate the pressure range for which the ejected sheet first breaks up into droplets. u_0^* indicates the transition between low-u_0 and high-u_0 regimes. Higher m_G (SF_6) lowers the curve but does not affect the trend in data. *Main*: Scaled threshold pressure, $P_T(m_G/m_{air})^{0.5}$, versus u_0 for the two gases, collapsing data in both regimes.

through ℓ as $\ell^{-1} \propto P m_G^{0.5}$ [16]. Since ℓ is inversely proportional to P, ℓ at the splash threshold is determined with the following relation:

$$\frac{\ell_T}{\ell_{atm}} = \frac{P_{atm}}{P_T} \tag{3}$$

where ℓ_T is the mean free path at P_T and ℓ_{atm} is the mean free path of He, air, or SF_6 at atmospheric pressure (P_{atm}=101 kPa) and room temperature (values found in [16,17]).

Using R/ℓ_T, Re, and We, I replot all data of Fig. 2(a) using axes that are rescaled to a dimensionless pressure and velocity (see Fig. 3):

$$P_T \rightarrow \left(\frac{R}{\ell_T}\right)^{1.0\pm0.2} \mathrm{Re}^{-0.5\pm0.08} \tag{4}$$

$$u_0 \rightarrow \mathrm{We}^{0.7\pm0.05} \mathrm{Re}^{-0.4\pm0.04} \tag{5}$$

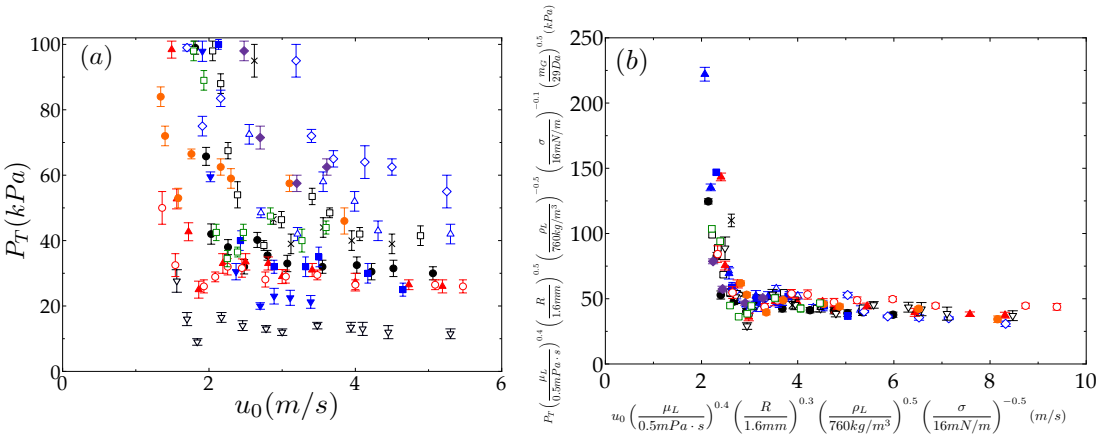

	△	◆	●	□	▼	◇	▲	▽	□	●	■	○	✖
μ_L (mPa·s)	0.5	0.8	1.1	1.2	1.2	1.7	1.7	1.7	1.8	1.8	2.1	2.3	2.7
R (mm)	1.6	0.8	1.6	0.9	0.9	1.6	1.6	1.6	0.8	0.8	2.0	1.6	1.0
σ (mN/m)	16.5	17.4	22.1	18.0	18.0	18.7	18.7	18.7	19.0	16.0	67.0	19.7	67.0
ρ_L (kg/m^3)	760	756	789	780	780	840	840	840	755	1860	1040	765	1070
m_G (Da)	29	29	29	29	146	4	29	146	29	29	29	29	29
ℓ (nm)	68	68	68	68	25	193	68	25	68	68	68	68	68

Fig. 2: (a) P_T vs. u_0, varying μ_L, R, σ, ρ_L, and m_G. Data sets correspond to symbols given in the table. (b) The data in both regimes collapse to one curve when P and u_0 axes are scaled as functions of μ_L, R, σ, ρ_L, and m_G as given in Equations 1 and 2 of the text.

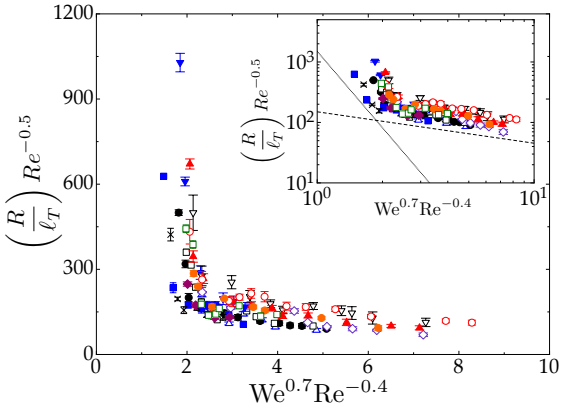

Fig. 3: Data are collapsed to a master curve by rescaling axes to functions of dimensionless numbers Re, We, and R/ℓ_T. Low-u_0 and high-u_0 regimes follow approximate power laws of -4.2 ± 0.85 and -0.52 ± 0.09, respectively, as shown in the inset plot of the data on a log-log scale.

The errors indicate the range over which this decent collapse is achieved. From the scaling of Fig. 2(b), the nearest collapse is found with dimensionless numbers, which encompass all physical quantities of the problem. I note that the collapse using dimensional variables (Fig. 2(b)) is better than that achieved with dimensionless quantities (Fig. 3). One clear reason for this can be attributed to the number of free parameters used in each case. In the collapse using dimensional numbers, six parameters are used whereas for the collapse with dimensionless variables, only half of the parameters are used; the relative simplicity of the collapse with dimensionless numbers is an achievement. It is possible to add additional dimensionless variables in order to improve the collapse. Although I have tried to include other parameters, the collapse achieved did not improve significantly.

Low-μ_L splash threshold measurements of other authors are shown in the inset plot of Fig. 4. The scaling applies whether the splash threshold is determined by varying solely Re and We at P_{atm} [6, 7], decreasing P [9], or increasing P above P_{atm} [12]. All data collapse to the master curve, as shown in the main plot of Fig. 4.

Splash correlations. – Figure 3 clearly highlights two distinct regimes in u_0 with the crossover occurring at u_0^*. From this curve, a splash criterion is found for each regime. First consider the low-u_0 regime, for which there is no previous scaling attempt. In this regime, the master curve approximately follows a power law of -4.2. The data therefore scales as $(R/\ell_T)\cdot\mathrm{Re}^{-0.5} \propto (\mathrm{We}^{0.7}\mathrm{Re}^{-0.4})^{-4.2}$ and can be simplified to the following relation:

$$\left(\frac{R}{\ell_T}\right)^{0.5\pm0.1} \mathrm{Re}^{-1.1\pm0.2}\mathrm{We}^{1.5\pm0.3} \approx 100 \qquad (6)$$

In Fig. 5(a), Eq. 6 at threshold pressure is presented as a function of P for the low-u_0 regime. The errors in

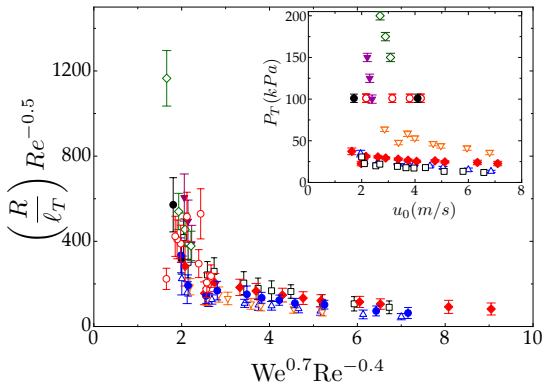

Authors	Symbol	μ_L (mPa.s)	ρ_L (kg/m3)	σ (mN/m)	Ambient Gas	R(mm)
Range and Feuillebois [6]	●	1 - 1.07	789 - 1000	22.1 - 1000	Air	1.9
Xu et.al. [9]	▽	0.54	792	22.6	Air	1.7
	●	1.07	789	22.1	Air	1.7
	△	1.07	789	22.1	Krypton	1.7
	□	1.07	789	22.1	SF6	1.7
	◆	2.1	804	23.8	Air	1.7
VanderWal et al. [7]	○	0.41 - 2.63	684-1080	20.1-72.8	Air	1.0
Mishra et al. [12]	◇	0.54	792	22.7	Air	1.05-1.3
	▼	1.07	789	22.1	Air	1.05-1.3

Fig. 4: *Inset*: $P_T(u_0)$ for published splash threshold data of other authors. Data sets correspond to symbols noted in table. *Main*: Data are scaled onto the master curve of the low-μ_L splash threshold.

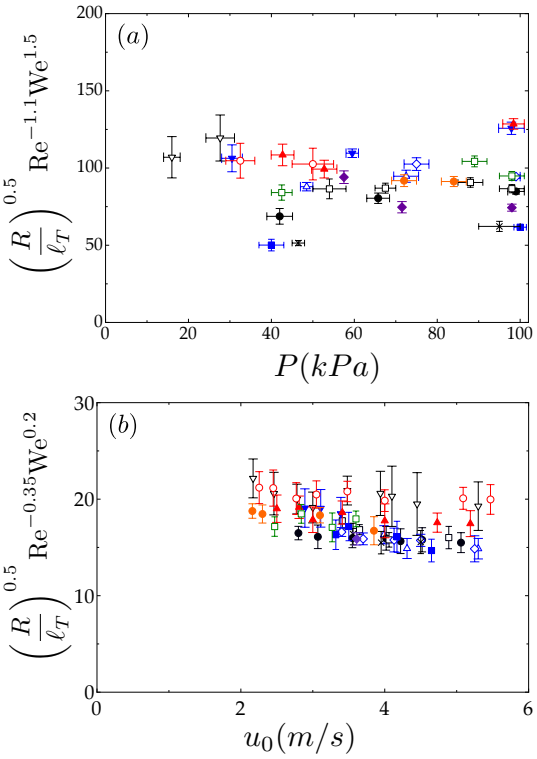

Fig. 5: Splash threshold criteria for (a) low-u_0 and (b) high-u_0 regimes. Data sets correspond to those of Fig. 2 and 3.

exponents are determined such that the average deviation of all data from the mean value is less than 25%. This correlation indicates that splashing is expected for values greater than the threshold.

The analysis is extended to the high-u_0 regime, where the curve approximately follows a power law of -0.52. The data scales as $(R/\ell_T)\cdot \mathrm{Re}^{-0.5} \propto (\mathrm{We}^{0.7}\mathrm{Re}^{-0.4})^{-0.52}$ and leads to the correlation at high-u_0:

$$\left(\frac{R}{\ell_T}\right)^{0.5\pm0.1} \mathrm{Re}^{-0.35\pm0.05}\mathrm{We}^{0.2\pm0.03} \approx 20 \qquad (7)$$

The errors are determined such that the deviation from the mean is within 10%. The threshold value for the splash transition in the high-u_0 regime is shown as a function of u_0 in Fig 5(b).

This new threshold is not the same as the previously proposed model by Xu *et al.* [9]. They derived an estimate based on variations to some, but not all, parameters. After varying all liquid control parameters, including σ, R, and ρ_L, a new threshold is found for this regime. For instance, a weaker effect of surface tension σ ($P \propto \sigma^{0.4}$ compared to $P \propto \sigma$) is found, though both criteria qualitatively show that higher σ inhibits splashing. There is also a weaker correlation with u_0; the dependence of P on u_0 is lower than was found by Xu *et al.* [9]. The proposed criterion does show the same dependence on m_G and gas temperature as expressed through ℓ_T.

Conclusions. – I provide a comprehensive study of low-μ_L drop impact on dry, smooth surfaces. The threshold pressure for splashing highlights two regimes in impact velocity u_0 with a crossover between them at u_0^*. Remarkably all data, over both regimes in u_0, can be rescaled onto a single curve, allowing us to define splash criteria approximately with only three dimensionless numbers: R/ℓ_T, Re, and We. A criterion is provided for the threshold in the low-u_0 regime, for which no data collapse was previously reported. A new scaling for high-u_0 is found.

All work reported in this paper focuses on the low-μ_L regime. Prior experiments describe a low-μ_L splash as the formation of an expanding sheet, which lifts up from the surface to a crown shape and becomes smaller at lower pressures [9]. This splash creation was proposed to result from air trapped under the drop upon impact [18, 19]. In the high-μ_L regime, a splash was shown to develop through thin sheet ejection from a thicker lamella; this thin sheet is ejected at later times with lower pressures [13, 20]. In addition to the low-μ_L splash thresholds presented here, it is valuable to find similar criteria for the velocity regimes at high viscosity. Such scaling estimates for the regimes in liquid viscosity can lead to theory of the basic mechanisms behind these different splashes.

* * *

I am particularly grateful to Sidney R. Nagel for his keen insight and valuable guidance throughout this work. I thank I. Bischofberger, J. Burton, T. Caswell, D. Devendran, M. Driscoll, A. Latka, I. Peters, and W. Zhang for helpful discussions. This work was supported by NSF

Grant DMR-1105145 and facilities of the University of Chicago NSF-MRSEC, supported by DMR-0820054. I also acknowledge support from the NSF Graduate Research Fellowship Program.

REFERENCES

[1] Worthington A. M., *Proc. R. Soc. London*, **25** (1876) 261-272.
[2] Tran T. *et al.*, *Phys. Rev. Lett.*, **108** (2012) 036101.
[3] Yarin A. L., *Ann. Rev. Fluid Mech.*, **38** (2006) 159-192.
[4] Stow C. D. and Hadfield M. G., *Proc. R. Soc. London*, **373** (1981) 419-441.
[5] Mundo C., Sommerfeld M., and Tropea C., *Int. J. Multiphase Flow*, **21** (1995) 2.
[6] Range K. and Feuillebois F., *J. Colloid Interface Sci*, **203** (1998) 16-30.
[7] Vander Wal R. L., Berger G. M., and Mozes S. D., *Exp. Fluids*, **40** (2006) 53-59.
[8] Rein M. and Delplanque J. P., *Acta Mech.*, **201** (2008) 105-118.
[9] Xu L., Zhang W. W., and Nagel S. R., *Phys. Rev. Lett.*, **94** (2005) 184505.
[10] Xu L., *Phys. Rev. E*, **75** (2007) 056316.
[11] Liu J. *et al.*, *Atomization and Sprays*, **20** (2010) 297-310.
[12] Mishra N. K., Zhang Y., and Ratner A., *Exp. Fluids*, **51** (2011) 483-491.
[13] Driscoll M. M., Stevens C. S., and Nagel S. R., *Phys. Rev. E*, **82** (2012) 036302.
[14] Latka A. *et al.*, *Phys. Rev. Lett.*, **109** (2012) 054501.
[15] Latka A., *Private Communication.*
[16] Lide D. R., *CRC Handbook of Chemistry and Physics*, **77** (1997) 6-52, 6-206.
[17] Marsh E. R. *et al.*, *Precision Engineering*, **32** (2008) 143-147.
[18] Mandre S., Mani M., and Brenner M. P., *Phys. Rev. Lett.*, **102** (2009) 134502.
[19] Mandre S. and Brenner M. P., *J. Fluid Mech.*, **690** (2012) 148-172.
[20] Driscoll M. M. and Nagel S. R., *Phys. Rev. Lett.*, **107** (2011) 154502.